

Reliability of Acoustic Emission as a Technique to Detect Corrosion and Stress Corrosion Cracking on Prestressing Steel Strands

Lamine Djeddi^{1,*}, Rabia Khelif^d, Salim Benmedakhene² and Jérôme Favergeon²

¹Mechanics of Materials and Plant Maintenance Research Laboratory (LR3MI), Badji Mokhtar-Annaba University, P.O. Box 12, 23000 Annaba, Algeria.

²Roberval Laboratory, UMR CNRS 6253, Research Centre of Royallieu, Technology University of Compiègne, BP 20529, F-60205 Compiègne, France.

*E-mail: djeddi.lamine@yahoo.fr

Received: 20 March 2013 / *Accepted:* 4 May 2013 / *Published:* 1 June 2013

Corrosion of prestressing strands is one of the main causes of deterioration of civil engineering structures, hence the need of monitoring these cables on real-time in order to avoid any accident. This experimental work was aimed at investigating the ability of acoustic emission (AE) technique for detection and monitoring of corrosion evolution and failure of strands. First, accelerated corrosion tests with ammonium thiocyanate were performed on a central wire cable without applied force and on a tensioned strand to 80% of guaranteed ultimate tensile strength have enabled to collect and to compare the acoustic responses of phenomena occurring during the corrosion of wire and cable, even those of phenomena very little emissive, such as rupture of the passive film. Then, an accelerated corrosion test under cathodic polarization until failure was achieved on a tensioned cable. Finally, the analysis of the failure process used the pattern recognition classification with Visual Class program. The results have shown that the fracture mechanism of the stress corrosion cracking process is associated with hydrogen absorption. It has been proven that AE is a very useful technique to detect and evaluate corrosion and failures of high-strength steel strands.

Keywords: Electrochemical corrosion, Stress corrosion cracking, hydrogen embrittlement, cathodic polarization, acoustic emission, prestressing strand.

1. INTRODUCTION

A very important part of physical infrastructure is formed by prestressed concrete structures like buildings, the transportation infrastructure, energy production, nuclear power plants, waste-water

treatment [1]. The development of early cracks in reinforced concrete due to incompatibility in the strains of steel and concrete was perhaps the starting point in the development of a new material like “prestressed concrete”. The application of permanent compressive stress to a material like concrete, which is strong in compression but weak in tension, increases the apparent tensile strength of that material, because the subsequent application of tensile stress must first nullify the compressive prestress. In 1904, Freyssinet attempted to introduce permanently action forces in concrete to resist the elastic forces developed under loads and this idea was later developed under the name of “prestressing” [2]. Prestressing of concrete is provided by pretensioning high tensile steel strands covered by their advantages including high tensile strength, lower weight and easy installation.

Prestressing creates stress or strain in a structure to prevent cracking and enhance durability and fatigue endurance, this durability is directly affected by the health of steel strands [3] Cementitious material constitutes a barrier against the ingress of aggressive substances to the steel surface. The high-alkaline pH of concrete pore solution around 12 keeps the steel in passive condition with an oxide passive film formed on the steel surface [4,5].

However, due to the excess of water necessary to maintain plasticity during mixing and casting of concrete, a greater or smaller porosity of the dry material results. The pores allow the diffusion of corrosive species like chlorides from the external environment, as in structures exposed to sea water or when de-icing salts are used on roads and bridges. Contaminants can move towards the prestressing strands promoting corrosion. Corrosive substances can be also introduced at the very moment of concrete implementation as when sea water is used in concrete mixing or when calcium chloride is used as a hydration accelerator. [6]

Main phenomena which lead to damage prestressing strands are pitting corrosion [7], stress corrosion cracking [8] and hydrogen embrittlement [9,10]. These phenomena cause a small reduction in load bearing area which can lead to reduced structural capacity and finally to deterioration of the civil engineering buildings [11,12]. In recent years, failures in high-strength steel tendons in prestressed concrete structures have become a serious problem; the development of techniques to detect and evaluate the failures in prestressed concrete structures in long-term service has become one of the most important issues for effective maintenance programs. [13].

To consider any accident, it is important to check the state of reinforcement steel during their lifetime. This state is often difficult to evaluate [14] in particular for the prestressing strands which are embedded in the concrete because of the great thickness of concrete surrounding them. Actually such an evaluation can be performed using two types of methods: intrusive methods and non-destructive methods. The first class is to be avoided, because it is necessary to break the concrete to have access to the strands; the excessive use of the intrusive methods causes a weakening of the structure. The non-destructive methods are thus favored, but a wise choice of a method among the large range of existing methods remains necessary. Among those, the acoustic emission is an interesting candidate for our study.

This paper is a continuation of our previous work on detection and characterization of corrosion on concrete reinforcements [15]. The present work aims to investigate the reliability of acoustic emission technique to detect and to characterize corrosion of prestressing strands steel used on the bridges, where we focused on three main objectives:

1. To achieve an accurate detection of strands corrosion process under the imposed electrochemical potential conditions by the use of acoustic emission technique.
2. To study correlations among obtained results and their relations to the corrosion process.
3. To carry out tests under cathodic polarization in order to modify the phenomena leading to the beginning of the damage.

2. EXPERIMENTAL

2.1. Acoustic emission technique

Acoustic emission (AE) has been developed for more than three decades as a non-destructive evaluation technique and as a useful tool for materials research.

The AE technique, based on the rapid release of energy from a localised source or sources within a material generating a transient elastic wave propagation, was demonstrated to be a very powerful and sensitive technique to monitor and study mechanisms of localised corrosion such as stress corrosion cracking [16], abrasion or erosion corrosion [17], and pitting corrosion [18] stress corrosion cracking [19], abrasion or erosion corrosion [20], pitting corrosion [21], crevice corrosion [22], exfoliation corrosion [23] and uniform “acidic” corrosion [24].

The Acoustic Emission non destructive technique (NDT) technique permits the detection and the conversion of high frequency elastic waves generated by the rapid release of energy to electrical signals. This is accomplished by directly coupling piezoelectric transducers on the surface of the structure under test. The output of each piezoelectric sensor (during structure loading) is amplified through a low-noise preamplifier, filtered to remove any extraneous noise and furthered processed by suitable electronic equipment.

The acoustic emission signal is characterized principally by the following parameters (Figure 1):

- Maximum amplitude (dB): maximum amplitude of the signal inside a salve.
- Duration (μs): time difference which separates the first and the last going beyond of the threshold.
- Energy (energy unit): integral of the amplitude square of the salve over all the duration of the signal.
- Rise time (μs): time difference between the first going beyond from the threshold and the maximum value of the signal amplitude.
- Counts (without dimension): number of times where the salve amplitude exceed the value of the threshold.
- The number of events “hit”: it is the counting of events having exceeded a threshold either during a time base, or throughout the test. In the first case, one speaks about rate of events, in the second of cumulated events.

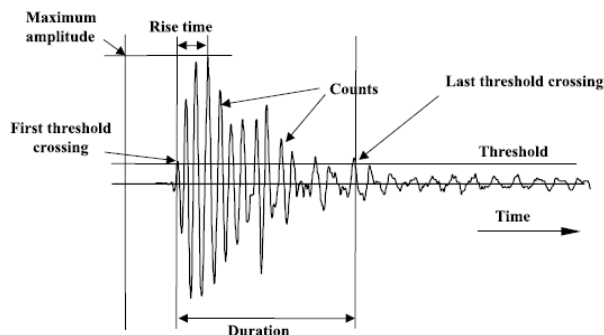


Figure 1. Example of an acoustic signal or salve, with definition of the shape parameters [25].

2.2. Strand description

This study is carried out on the commercially available prestressing steel strands T15,7. In this type of strand, six wires are spun around a central wire. The central wire is larger than the other wires. The steel used for these strands is obtained after cold wiredrawing.

Table 1. Steel chemical composition of T15,7 strand.

Element	C	Mn	Si	P	S
Composition [wt.%]	0.81	0.685	0.235	0.012	0.003

The composition of the steel prestressing strand is given in Table I. This strand has sketched in Figure 2, the radius of the central wire $R1 = 2.7\text{mm}$ and the radius of helical wires $R2 = 2.6\text{ mm}$, for a global section equals to 151.2 mm^2 . The main mechanical properties are given in Table II.

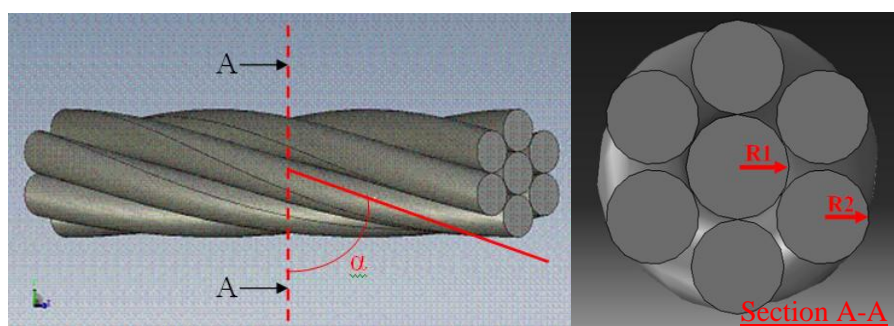


Figure 2. T15,7 strand geometry with a central wire and 6 helical wires.

Table II. Mechanical properties of T15,7 strand.

F0.1 [kN]	Fm [kN]	Elongation [%]
274	294.5	5.4

2.3. Electrochemical environment

The electrolyte used to perform steel corrosion was obtained by dissolving 250g of ammonium thiocyanate, NH_4SCN , in 1 liter of distilled water at room temperature.

A potentiostat using the VOLTAMASTER software was used for electrochemical experiments. Working electrode (WE) was made following the test, either central wire, or strand. Reference electrode, is a saturated calomel electrode (SCE). A platinum grid is used as counter electrode.

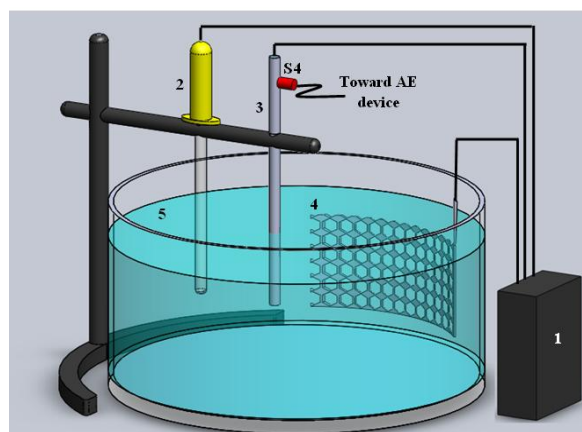
2.4. Acoustic emission monitoring system

In order to detect AE signals generated by chemical degradation and damage evolution, four sensors are used [15]; two PICO type sensors (S3, S4) which have a very good sensitivity and two 150 kHz resonance ultrasonic emission sensors, type VS150-M (S1, S5). PICO sensors have an operating Frequency Range 200-750 kHz and resonant Frequency 250 kHz (Ref V/(m/s)).

The sensors are connected to VALLEN AEP4 preamplifiers, with a programable gain fixed at 34 dB; the frequency bande extends from 20 kHz with 2 MHz. the AE acquisition device is the commercial VALLEN AMSY 4[®] system. The acoustic data processing is carried out using the VISUAL AE[®] software and the analysis of the waveforms is carried out with the VISUAL TR[®] software. To eliminate most of unwanted signals due to the external noise, the detection threshold of the AE signals was fixed at 30.6 dB.

The Reame Time is fixed at 2 ms; this parameter limits the duration of recorded salve. The Duration Discrimination Time is chosen as 100 μs which correspond to the duration which separates two consecutive salve records.

2.5. Accelerated corrosion tests



1: Potentiostat, 2: Reference electrode, 3: steel wire, 4: platinum grid, 5: NH_4SCN solution.

Figure 3. Experimental device used during the test 1.

To carry out this study, three kinds of tests were performed:

Test 1

In order to detect and identify the acoustic emission signals, which have only origin chemical phenomena related to corrosion, a central wire length of 20 cm was immersed in the ammonium thiocyanate solution, without mechanical effort applied. A potential scan was applied between -1200 mV/ SCE and -200 mV/SCE with a scanning rate of 8 mV/min. Electric current was measured, and a PICO AE sensor (S4) was placed on the wire, itself connected to the AE acquisition device (Figure 3).

Test 2

The principle of this test is to keep the cable 80% of its guaranteed ultimate tensile strength on a rigid frame. A corrosion cell was positioned around the cable and was filled with a corrosive solution containing ammonium thiocyanate in order to generate corrosion phenomena which will start damage of the strand.

Loading of the strand is provided by means of a hollow piston hydraulic cylinder; this cylinder is governed by a manual pump. A check valve is necessary to prevent the pressure drops. A potential scan is applied between -1200 mV/ECS and -200 mV/ECS with a scanning rate of 8 mV/min (Figure 4).

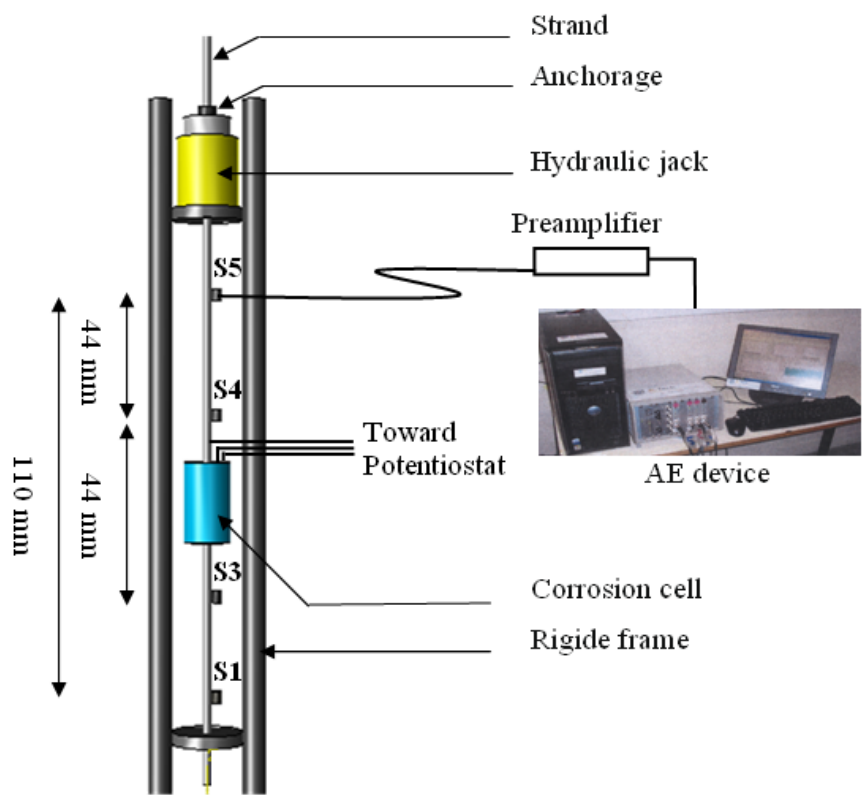


Figure 4. Experimental device used during the test 2 and test 3.

Test 3

During this test, we performed measurements under similar experimental conditions of Test 2, except that the potential scanning was carried out between -800 mV and -400 mV with a scanning rate of 3 mV / min, then the potential was maintained at -400 mV until break of one or more wires.

This SCC test was performed at constant load; when a crack starts or spreads the effective section of the strand decreases locally, the stress intensity increases at the front of the crack. These tests are more stringent than the tests at constant strain.

3. RESULTS AND DISCUSSION

A part of the central wire of the strand was immersed for 5 hours in the electrochemical solution NH₄SCN, the values of the free potential collected is -772 mV/SCE (Figure 5).

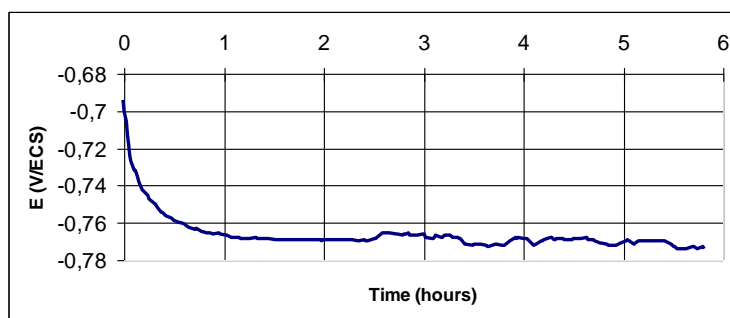


Figure 5. Evolution of open circuit potential with time of the steel in 20 wt% of NH₄SCN.

Figure 6 shows the variation of electric current with time of test 1 as well as the values of the maximum amplitude of each EA salve detected during acoustic monitoring of the wire. Three domains are distinguished; a cathodic zone (A), a passivity zone, (B) and an anodic zone (C).

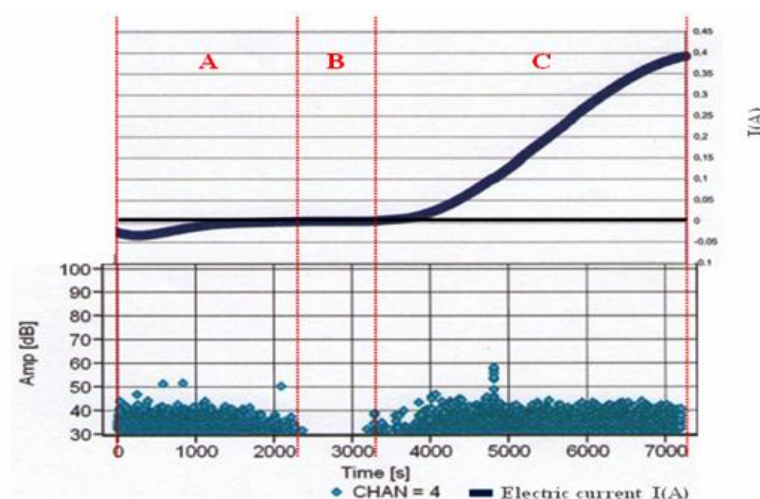


Figure 6. AE signals amplitudes versus time and polarization curve of the steel in 20 wt% of NH₄SCN at room temperature during test 1.

The cathodic zone (A) is characterized by a negative electric current, hydrogen ions are reduced to produce hydrogen gas, recorded AE signals can be attributed to the hydrogen evolution (Figure 7), or friction among hydrogen bubbles or the absorption of hydrogen by metal promoted by the presence of thiocyanate [26]. During the passivity of the steel (B), the electrical current becomes null, a protective layer is formed around the wire to prevent corrosion of the wire which explains the absence of an acoustic activity.

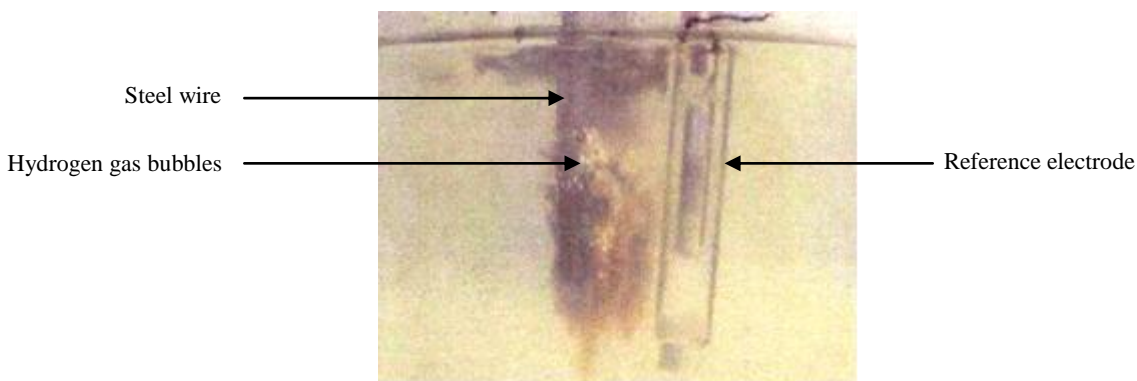


Figure 7. Hydrogen gas evolution of the wire.

A positive current (zone C) causes the reappearance of acoustic activity, with AE signal amplitudes almost equal to those of zone (A), these amplitudes remain constant with the increase of electric current. To determine the origin of these signals, an analysis of the energy and counts number was performed (Figure 8 and 9).

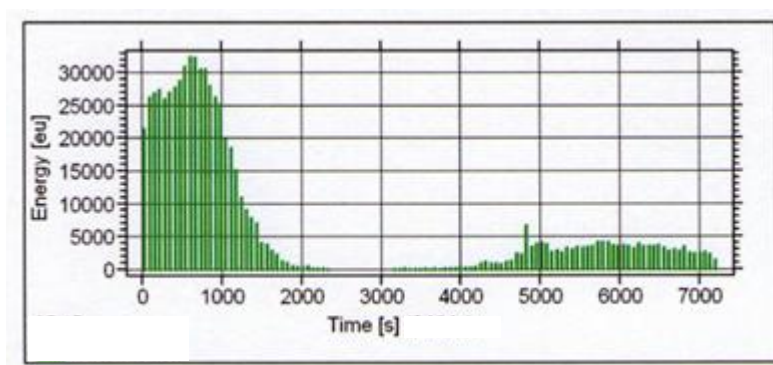


Figure 8. History plots of energy during time of test 1.

It turns out that the signals detected in the anodic zone are divided into two categories; the first one appears immediately after passivity, these signals have a very low energy and a high counts number suggesting that these signals have as origin a mechanical damage which could correspond to

the breakdown of the passive layer. The second category appears after 5000 seconds, the low energy of these salves let think that corrosion is the phenomenon which generates AE signals according to the results obtained by Jomdecha et al. [27].

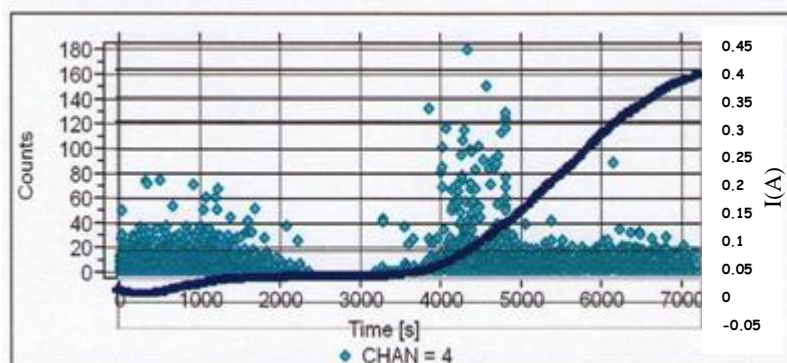


Figure 9. AE hits counts versus time and polarization curve of the steel in 20 wt% of NH_4SCN at room temperature during test 1.

Relevant characteristic parameters of salves, listed in Table III, allow us to represent distinctly populations signals appeared during test 1 (Figure 10).

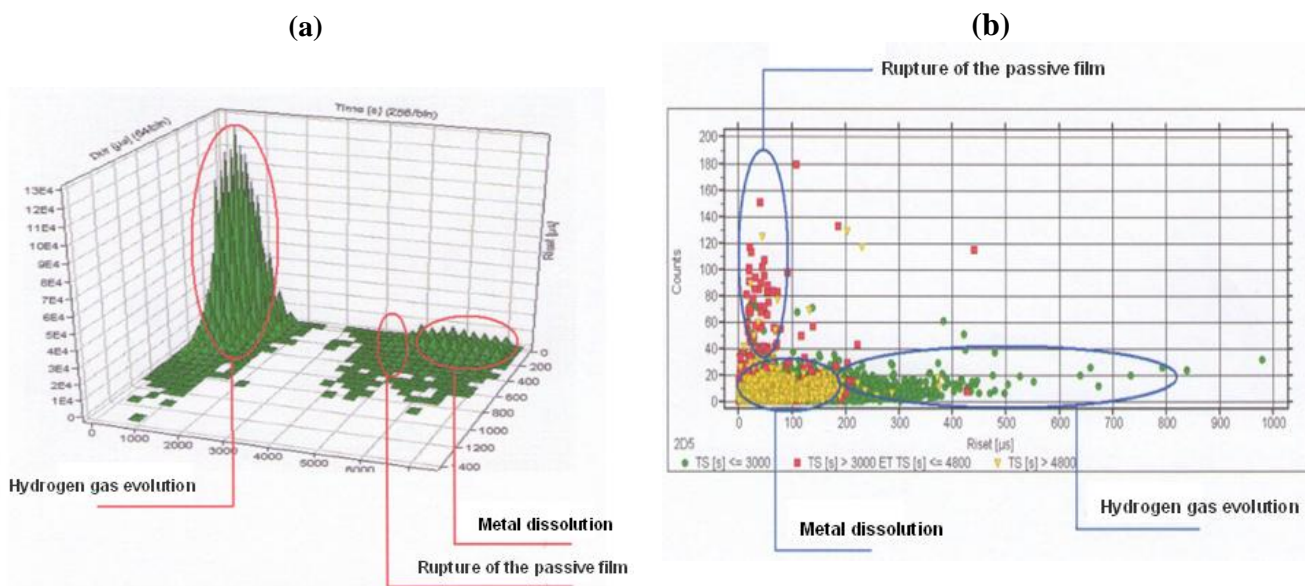


Figure 10. (a) 3D plot of acoustic parameters (duration, rise time) versus time during test 1. (b) AE hits counts versus rise time recorded during test 1.

The typical waveforms of each of these three signal populations and their frequential signature obtained by Fourier transform are presented on Figure 11.

Table III: Characteristics of acoustic signals linked to different phenomena during test 1

Sources of AE signals	Maximum amplitude (dB)	Rise time (μ s)	Counts	Energy [e.u.]
Hydrogen gas evolution	30.6-52	1-320	1-45	1- 200
Rupture of the passive film	30.6-45	1-47	1-160	1- 50
Steel dissolution	30.6-47	1-200	1-40	1-180

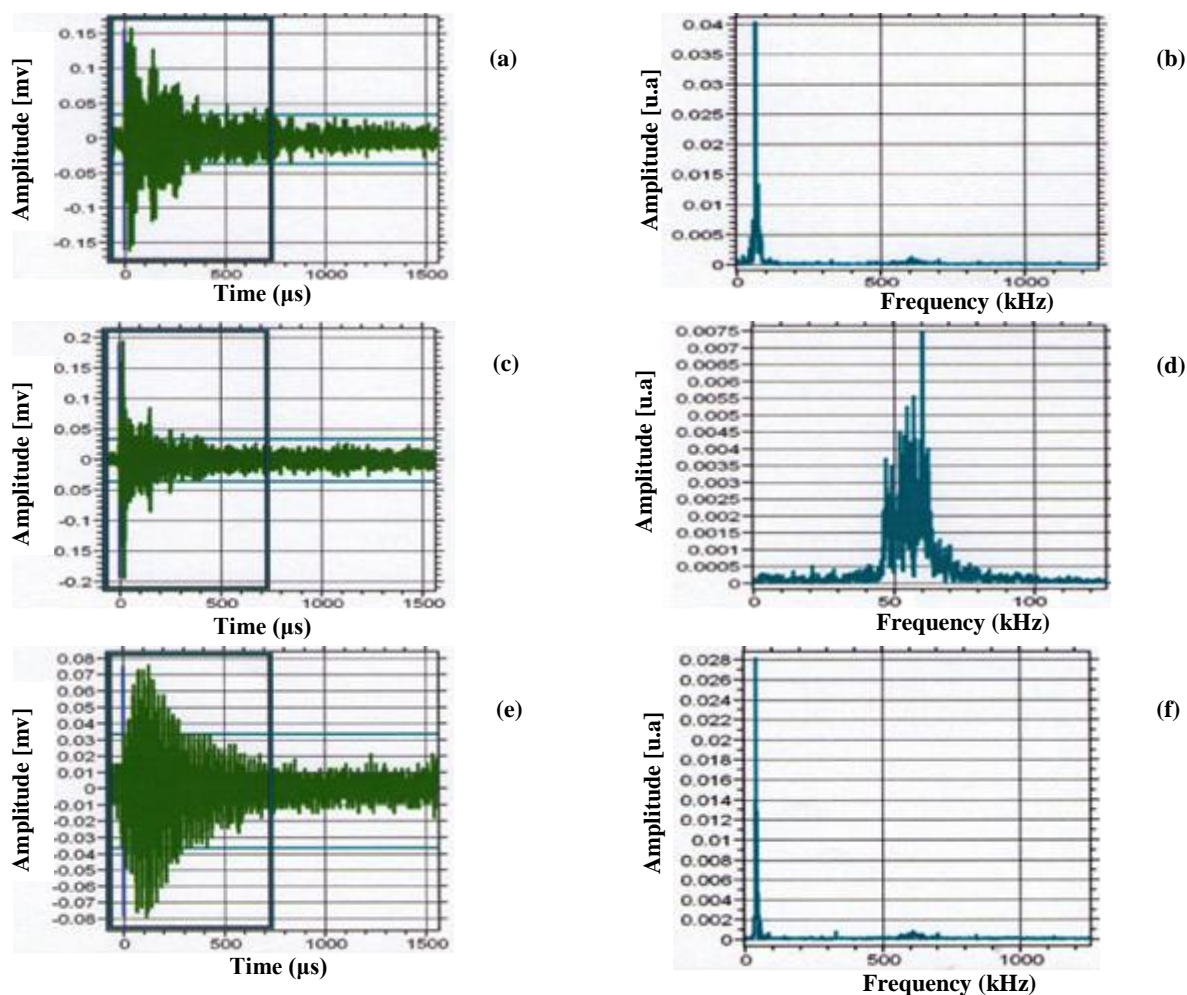


Figure 11. (a) Typical AE waveform observed during hydrogen gas evolution, (b) Frequency spectrum of AE signal during hydrogen gas evolution, (c) Typical AE waveform observed during rupture of the passive film, (d) Frequency spectrum of AE signal during passive film, (e) Typical AE waveform observed during metal dissolution, (f) Frequency spectrum of AE signal during metal dissolution.

Figure 12 shows the values of maximum amplitudes of the signals recorded during test 2; it appears an important acoustic activity in the cathodic field (till 1800 s), a strong release of hydrogen was observed. It can be seen that there were no AE Salves during passivity of the strand (1800s < t < 3000s). Salves detected in the anodic field (t > 3000s) are spaced and have constant average values of amplitude and a low energy highlighting the existence of a phenomenon which progresses slowly. The

breakdown of passive layer do not emit AE of detectable energy in experiment 2, this can be explained by the large distance between the solution and the sensors.

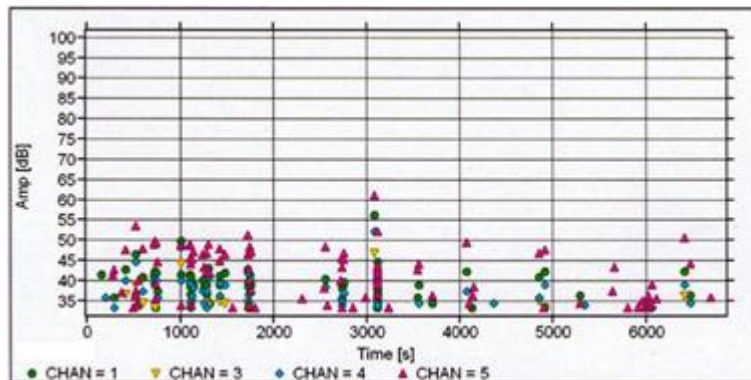


Figure 12. AE hits amplitude versus time recorded during test 2.

It is noticed that characteristic values of AE signals recorded during test 2 (listed in Table IV.) are close to the values obtained during the test 1 (Figure 13). These values characterize the phenomena causing acoustic activity; the presence of signals having as source a mechanical damage is therefore unlikely even if a traction force is applied.

Table IV: Characteristics of acoustic signals recorded during test 2

Sources of AE signals	Maximum amplitude (dB)	Rise time (μ s)	Counts	Energy [e.u.]
Cathodic field	30.6-54	1-325	1-45	1- 149
Anodic field	30.6-48	1-189	1-37	1- 141

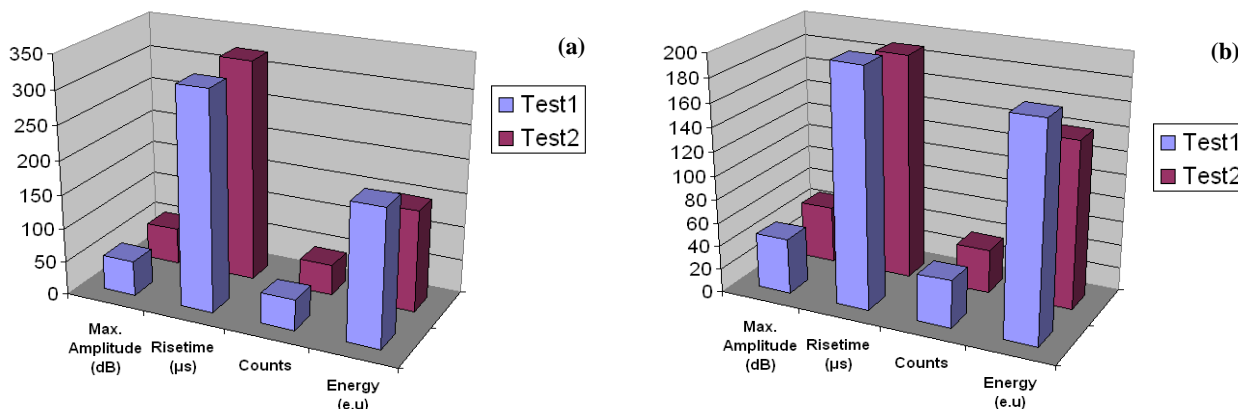


Figure 13. Statistical result of acoustic parameters (amplitude, rise time, counts and energy) of signals recorded during test 1 and test 2. (a) Cathodic field, (b) Anodic field.

It is noticed that the acoustic activity in the period $1000s < t < 1800s$ is more dense compared to the acoustic activity recorded in the period $t < 1000s$, this has led to an increase of the cumulated

number of counts at $t = 1000s$ (Figure 14). This means that in addition to the release of hydrogen observed, there is another process responsible for signals recorded in the cathodic field ($t < 1800s$). In order to identify this process, further investigations in the cathodic domain was performed (Test 3).

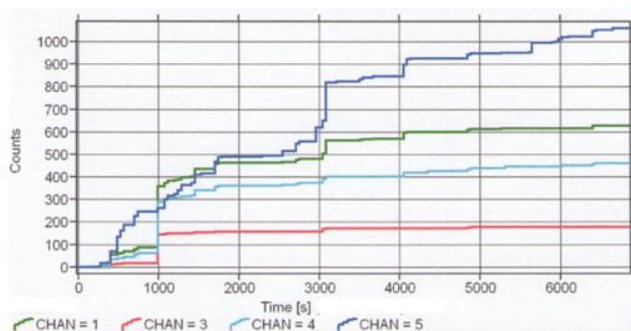


Figure 14. Evolution of cumulated number of counts versus time recorded during test 2 by each sensor.

Figure 15 gives the amplitude of the AE salves recorded throughout the test 3. The cable rupture occurs at about 15800 seconds of the test. It is noticed that acoustic activity remains weak during the first part of this test, and then it starts to become important after 5000 seconds. However, we did not observe an increase in the amplitude of signals until 12000 seconds. In the other hand, a dramatic increase in the amplitude of signals appears approximately 1800 seconds before the rupture of the strand.

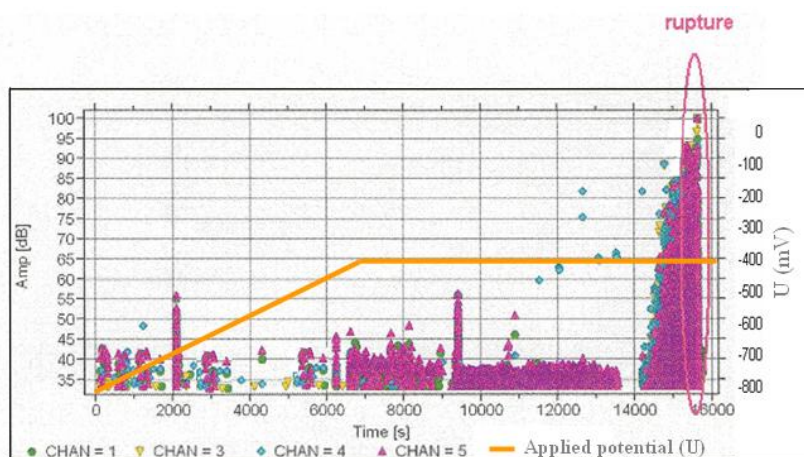


Figure 15. AE signals amplitudes versus time and values of imposed potential during test 3.

The signals waveforms recorded during test 3 were analyzed using unsupervised classification to differentiate various sources of AE signals; this led us to the application of a frequency domain pattern recognition system “Visual ClassTM” for the statistical classification of AE signals.

Visual class uses short time spectra for the classification of waveforms. The Figure 16 Shows a waveform and the coloured horizontal bars indicate the position of time windows. The content of each

time window is cut out using a Hamming window and its spectrum is calculated via a Fast Fourier Transform (FFT). The resulting Fourier points are called “features”. These features can be interpreted as the dimensions of a multidimensional space in which each waveform is represented by a single point. The hamming function is used to cut a part of the waveform. In order not to suppress information at the end and beginning of the window, the time windows overlap. [28]. These features are used to separate different classes of waveform.

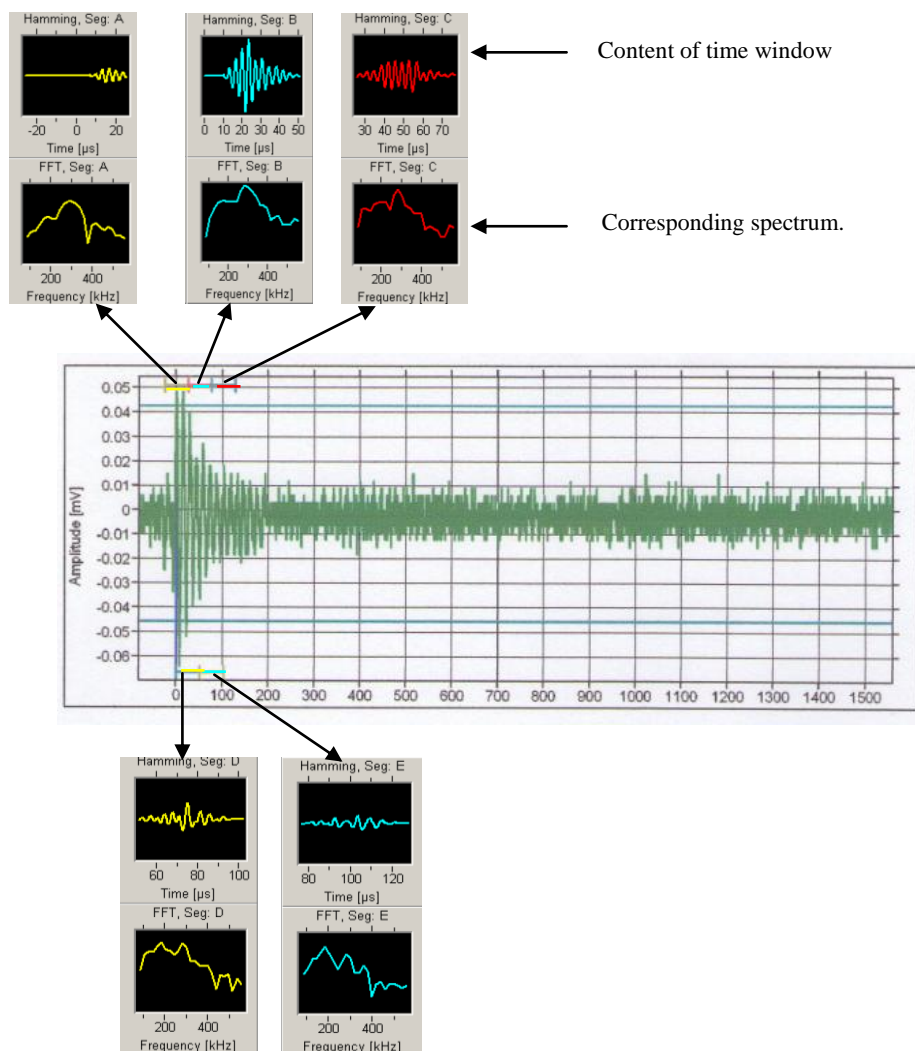


Figure 16. Frequency Spectra from Waveform Time Segments

Three classes (designated by colours blue red and green) were thus obtained (Figure 17). The phenomena corresponding to each class were determined by comparing the typical parameters of AE signals of each class to some published results of experiments works made for prestressing steel strands Subjected to stress corrosion cracking [7,13,26,29]. (In this case, the most important parameters of AE signals are expressed by the values of signals amplitude, frequency, and duration):

- Class 1 (blue) : Hydrogen penetration.
- Class 2 (red) : Hydrogen gas evolution.
- Class 3 (green) : Crack propagation and rupture.

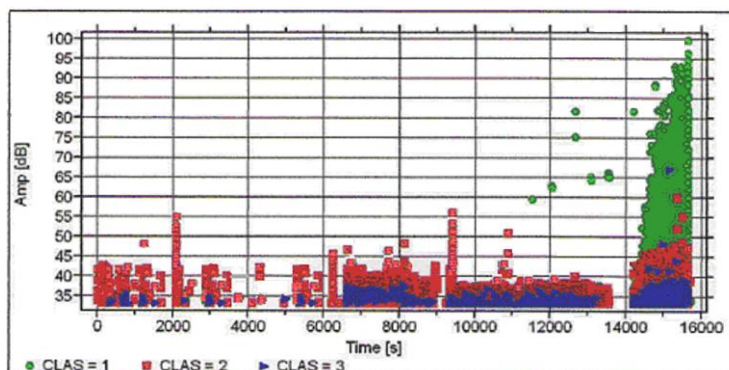


Figure 17. AE results for separated class: Amplitude versus. Time. Class 1 to 3 are indicated.

During the first stage of test3, acoustic activity is caused mainly by the evolution of hydrogen bubbles, corrosion products are formed on the wire surface. The amplitudes of signals caused by hydrogen absorption inside the metallic matrix do not exceed 35 dB. When the imposed potential attained -450 mV acoustic activity becomes denser, this is due to the delamination of thin metal layers on the wire surface which makes the cable more susceptible to corrosion, hydrogen atoms penetrate deeper in the steel causing its brittleness. This delamination is favored by the accumulation of hydrogen in the first micrometers of the steel according to Gaillet *et al.* [26]. Microcracks appear during this stage, but this mechanism does not emit AE of detectable energy in our experiment. Finally, during Step 3, hydrogen absorption inside the metallic matrix reaches a critic depth and cracks propagate causing rupture of the wire.

High amplitudes appear several minutes before the final rupture of the cable. These amplitudes have been noticed by many authors [26, 29,30].

4. CONCLUSIONS

The monitoring by acoustic emission technique of accelerated corrosion tests using ammonium thiocyanate allowed determining the characteristics of AE signals, corresponding to various degradation states of the prestressing strand. The characteristics of the signals having for origin chemical phenomena such as metal dissolution or diffusion of hydrogen bubbles do not vary significantly by applying or not a load on the cable.

Cathodic polarization has led to mechanical damage of the strand. The rapid crack propagation was detected approximately 30 minutes before the breakdown of the strand, which resulted in a sharp increase in AE signals amplitude.

The pattern recognition analysis technique allowed us to detect hydrogen penetration inside the metallic structure.

References

1. J. Kováč, M. Leban and A. Legat, *Electrochim. Acta*, 52 (2007) 7607.
2. N. Krishna Raju, *Prestressed Concrete*, 4th Edition Tata Mc Graw Hill Education, New Delhi, (2006).
3. Z. Liu, S. Liu, B. Wu, Y. Zhang and C. He, *Acta Mech. Solida Sin.*, 21 (2008) 573.
4. D. A. Hausmann, *Mater. Prot.*, 6 (1967) 19.
5. V.K. Gouda, *Brit. Corros. J.*, 5 (1970) 198.
6. R.M. Schroeder and I.L. Müller, *Corros. Sci.*, 45 (2003) 1969.
7. L. Fumin, Y. Yingshu, L. Chun-Qing, *Constr. Build. Mater.*, 25 (2011) 3878.
8. G.E. Monfore and C.J. Verbeck, *J. Am. Concr. Inst.*, 37 (1960) 491.
9. R.M. Schroeder and I.L. Müller, *Corros. Sci.*, 45 (2003) 1969.
10. S. Q. Wang, D. K. Zhang, D. G. Wang, L. M. Xu¹ and S. R. Ge, *Int. J. Electrochem. Sci.*, 7 (2012) 7376.
11. C. Zheng, G. Yi and Y. Gao, *Int. J. Electrochem. Sci.*, 7 (2012) 9518.
12. F. J. Olguin Coca, M. U. Loya Tello., C. Gaona-Tiburcio, J. A. Romero¹, A. Martínez-Villafañe E. Maldonado B, F. Almeraya-Calderón, *Int. J. Electrochem. Sci.*, 6 (2011) 3438.
13. S. Yuyama, K. Yokoyama, K. Niitani, M. Ohtsu and T. Uomoto, *Constr. Build. Mater.*, 21 (2007) 491.
14. H. W. Song, V. Saraswathy, *Int. J. Electrochem. Sci.*, 2 (2007) 1.
15. J. Favergeon, S. Benmedakhene, L. Djeddi and G. Moulin, *Ann. Chim.-Sci. Mat.*, 33(2008) 99.
16. Mazille H and Rothéa R, *The use of acoustic emission for the study and monitoring of localized corrosion phenomena*. In: K.R. Tretheway, P.R. Roberge, *Modelling aqueous corrosion*, Kluwer Academic Publishers, Netherlands, (1994).
17. F. Ferrer, H. Idrissi, H. Mazille, P. Fleischmann and P. Labeeuw, *Wear*, 231 (1999) 108.
18. A. Arora, *Corrosion*, 40 (1984)459.
19. S. Yuyama, T. Kishi and Y. Hisamatsu, *J.A.E.*, 2 (1983) 71.
20. M. M. El Rayes, H. S. Abdo, and K. A. Khalil, *Int. J. Electrochem. Sci.*, 8 (2013) 1117.
21. H. Mazille, R. Rothea and C. Tronel, *Corros. Sci.*, 37 (1995) 1365.
22. Y.P. Kim, M. Fregonese, H. Mazille, D. Feron and G. Santarini, *NDT&E Int.*, 36 (2003) 553.
23. F. Bellanger, H. Mazille and H. Idrissi, *NDT&E Int.*, 35 (2002) 385.
24. L. Jaubert, M. Fregonese, D. Caron, F. Ferrer, C. Franck, E. Gravy, P. Labeeuw, H. Mazille and L. Renaud, *Insight*, 47 (2005) 465.
25. F. Ferrer, T. Faure, J. Goudiakas and E. Andrès, *Corros. Sci.*, 44 (2002) 1529.
26. M. Perrin, L. Gaillet, C. Tessier and H. Idrissi, *Corros. Sci.*, 52 (2010) 1915.
27. C. Jomdecha, A. Prateepasen, and P. Kaewtrakulpong, *NDT&E Int.*, 40 (2007) 584.
28. M. J. Peacock, 30th European Conference on Acoustic Emission Testing & 7th International Conference on Acoustic Emission, *University of Granada*, 12-15 September (2012).
29. S. Ramadan, L. Gaillet, C. Tessier and H. Idrissi, *Appl. Surf. Sci.*, 254 (2008) 2255.
30. K. Y. Sung, I.S. Kim and Y.K. Yoon, *Scripta Mater.*, 37 (1997) 1255.